CDF Note 9221

Multivariate Likelihood Search for Single-Top-Quark Production with 2.2 fb^{-1}

The CDF Collaboration
URL http://www-cdf.fnal.gov
(Dated: February 28, 2008)

We report results from the multivariate likelihood function search for single-top production with CDF II data corresponding to 2.2 fb^{-1} of integrated luminosity. The best-fit value for the combined s+t-channel production of single-top quarks assuming the Standard Model ratio of their production cross sections is $\sigma_s + \sigma_t = 1.8^{+0.9}_{-0.8}$ pb.

Preliminary Results for Winter 2008 Conferences

I. INTRODUCTION

According to the Standard Model, in $p\bar{p}$ collisions at the Tevatron top quarks can be created in pairs via the strong force, or singly via the electroweak interaction. The latter production mode is referred to as "single-top-quark" production and takes place mainly through the $s-$ or $t-$ channel exchange of a W boson (Figure 1). Both the CDF and DØ collaborations have reported single-top results using $\sqrt{s} = 1.96$ with approx. 1fb^{-1} of data, and the DØ collaboration has published 3σ evidence for single-top[13, 14].

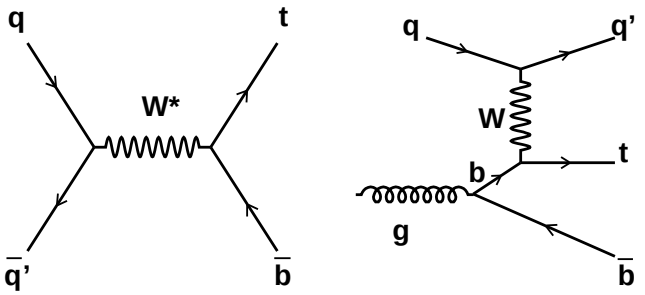

FIG. 1: Representative Feynman diagrams for single-top-quark production at the Tevatron: s-channel W^* (left) and t-channel W-gluon fusion (right).

Studying single-top production at hadron colliders is important for a number of reasons. First, it provides a direct window into measuring the CKM matrix element $|V_{tb}|^2$, which is closely tied to the number of quark generations. Second, measuring the spin polarization of single-top quarks can be used to test the V-A structure of the top weak charged current interaction. Third, single-top events represent an irreducible background to several searches for SM or non-SM signals, for example Higgs boson searches. Fourth and last, the presence of various new SM and non-SM phenomena may be inferred by observing deviations from the predicted rate of the single-top signal.

The theoretical single-top production cross section is $\sigma_{s+t} = 2.9$ pb for a top mass of 175 GeV/c^2 [3]. Despite this small rate, the main obstacle in finding single-top is in fact the large associated background. After all section requirements are imposed, the signal to background ratio is close to 1/15, and the systematic uncertainties on the background are on the order of 20% This challenging, background-dominated dataset is the main motivation for using multivariate techniques. The following sections present the event selection, the signal and background estimations, an extended b-tagger and a kinematic solver used to improve signal identification, the statistical techniques, the expected and observed single-top cross section results, and a brief summary of these results.

II. SELECTION REQUIREMENTS

Our selection exploits the kinematic features of the signal final state, which contains a top quark, a bottom quark, and possibly additional light quark jets. To reduce multijet backgrounds, the W originating from the top quark is required to have decayed leptonically. We demand therefore a high-energy electron or muon ($E_T(e) > 20$ GeV, or $P_T(\mu) > 20$ GeV/c) and large missing energy from the undetected neutrino $\not\!\!E_T$>25 GeV (using jets corrected to the hadron level). We reject dilepton events from $t\bar{t}$ and Z decays, by requiring the dilepton mass to be outside the range: 76 GeV/c^2 < $M_{\ell\ell}$ < 106 GeV/c^2. The backgrounds surviving these selections can be classified as "non-top" and $t\bar{t}$. The non-top backgrounds are: $Wb\bar{b}$, $Wc\bar{c}$, Wc, mistags (light quarks misidentified as heavy flavor jets), non-W (events where a jet is erroneously identified as a lepton), and diboson WW, WZ, and ZZ. We remove a large fraction of the non-top and $t\bar{t}$ backgrounds by demanding exactly two "tight" jets with $E_T > 20$ GeV (corrected to hadron level) and $|\eta| < 2.8$ be present in the event. At least one of the two tight jets should be tagged as a b-quark jet by using displaced vertex information from the silicon vertex detector (SVX). The non-W content of the selected dataset is further reduced by imposing a set of requirements on i) transverse mass of the reconstructed W boson, ii) the $\not\!\!E_T$ significance (electron events only), and iii) the angle between the $\not\!\!E_T$ vector and the transverse momentum vector of the leading jets (electron events only).

TABLE I: Background estimates used in this analysis, along with the observed total (last row). The systematic uncertainties on these predictions, as used in the interpretation of the results, are given in Tables II,III and IV.

Process	2-jet Prediction	3-jet Prediction
t-chan	52.0 ± 7.6	15.1 ± 2.2
s-chan	34.0 ± 4.8	10.9 ± 1.6
$t\bar{t}(\ell + \text{jets})$	76.9 ± 11.0	232.2 ± 33.1
$t\bar{t}$ dilepton	39.1 ± 5.6	32.2 ± 4.6
$Wb\bar{b}$	425.9 ± 128.4	124.3 ± 37.5
$Wc(\bar{c})$	366.2 ± 112.9	95.2 ± 29.3
W+LF	309.5 ± 51.5	89.5 ± 15.1
Z+jets	20.0 ± 3.0	7.7 ± 1.1
WW	37.4 ± 4.1	12.7 ± 1.4
WZ	17.7 ± 1.4	5.0 ± 0.4
ZZ	0.5 ± 0.0	0.2 ± 0.0
non-W	57.1 ± 22.8	20.9 ± 8.4
Total	**1436.1 ± 248.5**	**645.9 ± 78.1**
Observed	**1396**	**591**

III. SIGNAL AND BACKGROUND ESTIMATIONS

We require rate and kinematic shape predictions for each background source separately with minimal systematic uncertainty in order to test for single top quark production. For some background sources, we are able to use the observed data to constrain their rates and test their shapes, using carefully constructed control samples. Other backgrounds must be estimated with Monte Carlo predictions scaled to theoretical calculations. The $t\bar{t}$, diboson (WW, WZ and ZZ) contributions, and $Z \to \ell\ell$ are estimated from theoretical predictions. The same can be said about signal estimations.

The background processes for which we can use CDF data to constrain rates and shapes are: W+heavy flavor ($Wb\bar{b}$, $Wc\bar{c}$, Wc), mistags, and non-W events. Their contributions are obtained using a similar method with that employed in Ref [4], with a few differences. One difference is the larger η range for the jet definition ($|\eta| < 2.8$) used in this search. The other difference is that a scale factor for the heavy flavor fraction is used, calculated using taged W+1 jet data.

The expected and observed event yields corresponding to the 2.2 fb^{-1} dataset are given in Table I, for both Monte-Carlo based and data based-background estimates.

IV. SPECIAL EVENT VARIABLES

A. ANN extended B-tagger

An Artificial Neural Network (ANN) [5] was developed to increase the b-quark purity of the sample selected by the standard $b-$tagging algorithm. The latter is based on measuring displaced (secondary) vertices, and in addition to b-jets it also selects a significant fraction of $c-$ and light flavor jets (as much as 50%). The extended (ANN) tagger is applied to jets selected by the standard b-tagger, and exploits mainly the long lifetime (1.6 ps) of b-hadrons. Other features used by the ANN are the high b-quark mass, the high decay multiplicity, and the decay into leptons. For illustration, Fig. 2 shows good shape agreement between the ANN output distributions for the $W + 2$ jet data and a sum of the individual background components normalized to data.

B. Kinematic Solver

We can use the measured momenta of the final state particles to reconstruct the W boson and the top quark, and constrain the reconstructed masses $M_{\ell\nu}$ and $M_{\ell\nu b}$ to 80.4 GeV and 175 GeV, respectively. The constraint of the event kinematics to these known masses improves the reconstruction of signal events, worsens the reconstruction of background events, and aids in the separation of the single-top signal from the background. The widths of the top quark and W boson mass distributions at the parton level are of the order of 2 GeV. At reconstructed level the

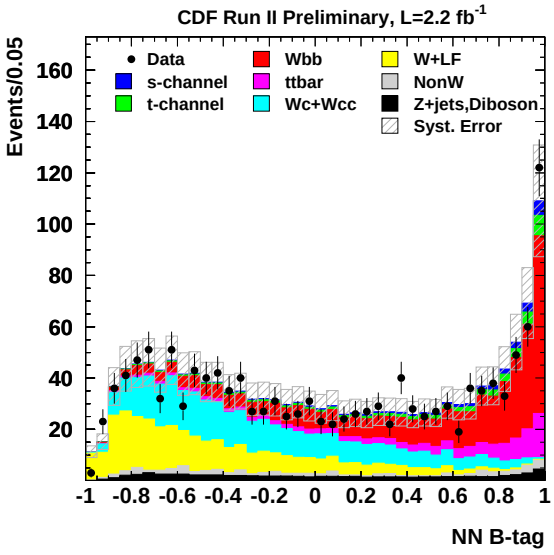

FIG. 2: The ANN tagger output distributions for the CDF W+2 jets events (points) compared to the Monte Carlo expectations.

measurement uncertainties are much larger, of the order of 20-40 GeV for $M_{\ell\nu b}$, if one were to use the reconstructed values in the t and s channels, respectively.

The kinematic constraints' use is twofold. First, the χ^2, which is constructed out of the difference between the *measured* jet energies, angles and $\not\!\!E_T$ and those required by the kinematic constraints, can be used instead of the reconstructed $M_{\ell\nu b}$ as a variable which helps separate signals from backgrounds. The second use of the kinematic constraints is to ensure that the input to the matrix element calculation has four-vectors which correspond to on-shell W bosons and top quarks.

An inventory of the constraints used is as follows:

- The lepton momentum vector is constrained to its measured value.
- The p_T of the top quark is constrained to its measured value.
- The direction and mass of the b jet from top decay are constrained to their measured values.
- $M_{\ell\nu}$ is constrained to 80.4 GeV, resulting in a second-degree equation with two neutrino p_z solutions.
- $M_{\ell\nu b}$ is constrained to 175 GeV.

These constraints are sufficient to solve for the energy of the b jet from top decay, with no regard to its measured value. The ambiguity choices – two possible assignments of the b-jet from top decay, and two neutrino p_z solutions (usually), means that the kinematic interpretation must be done four times.

The output from the kinematic solver is a set of neutrino and b-jet four-vector solutions, which are used to reconstruct kinematic variables. Also provided is the χ^2 output mentioned above, which indicates how far from the measured values of the b-jet energy and the $\not\!\!E_T$ the solver found its solutions. If the wrong choice of b-jet from top is made, then the χ^2 is typically worse than if the correct choice is made, and thus the χ^2 variable can be used to select the b jet in events in which the choice is ambiguous. The χ^2 definition is

$$\chi^2 = \frac{(E_b^{\rm solved} - E_b^{\rm meas})^2}{\sigma_b^2} + \frac{(M_{\ell\nu b} - 175GeV)^2}{\sigma_{m_t}^2} + \frac{(\Delta\not\!\!E_T)^2}{\sigma_{\not\!\!E_T}^2}, \quad (1)$$

where σ_b is taken to be 9 GeV, σ_{m_t} is taken to be 1 GeV, and $\sigma_{\not\!\!E_T}$ is taken to be 11 GeV.

V. LIKELIHOOD FUNCTION TECHNIQUE

No single variable encodes all conceivable signal-background separation, and so a likelihood function [6] is proposed to combine several variables together into a discriminant which can be used to compute limits or to discover a signal.

The likelihood function $\mathcal{L}$ is constructed by first forming histograms of each variable (n_i bins per variable), separately for the signal distributions and for several background distributions, denoted f_{ijk} for bin j of variable i for the event class k. For the signal, $k = 1$, and in this note, four background classes are considered: $Wb\bar{b}$, $t\bar{t}$, $Wc\bar{c}/Wc$, and mistags, which are event classes 2, 3, 4 and 5. These histograms are normalized such that $\sum_{j=1}^{n_i} f_{ijk} = 1$ for all i and all k. The likelihood function for an event is computed by evaluating in which bin j_i in which the event falls in the distribution of variable i, and computing

$$p_{ik} = \frac{f_{ij_ik}}{\sum_{m=1}^{5} f_{ij_im}}, \tag{2}$$

which is used to compute

$$\mathcal{L}_k(\{x_i\}) = \frac{\prod_{i=1}^{n_{var}} p_{ik}}{\sum_{m=1}^{5} \prod_{i=1}^{n_{var}} p_{ik}}. \tag{3}$$

The signal likelihood function is the one which corresponds to the signal class of events, $\mathcal{L}_1$.

Two likelihood functions are computed – $\mathcal{L}_t$ using the t-channel single-top signal in the signal reference histograms, and $\mathcal{L}_s$ using the s-channel single-top signal in the signal reference histograms. Plots of all input variables can be found on the Likelihood Function search public page [15].

A. t-channel Likelihood Function, 2 jet bin

The 2-jet bin t-channel likelihood function, $\mathcal{L}_t$, uses seven variables, and assumes the b-tagged jet comes from top decay. For doubly-tagged events, we set $\mathcal{L}_t = 0$. The 2-jet bin t-channel likelihood function uses the following seven variables:

- H_T, the scalar sum of the transverse energies of the two tight jets, the lepton, and the missing transverse energy.
- $Q \times \eta$, the charge of the lepton times the pseudorapidity of the tight jet which is not b-tagged.
- χ^2_t, output from the kinematic solver for the t-channel combination described above.
- $\cos\theta_{t-\mathrm{chan}}$, the cosine of the angle between the lepton and the untagged tight jet in the top decay frame.
- M_{jj}, the invariant mass of the two tight jets.
- $\log(\mathrm{ME}_{t-\mathrm{chan}})$, the logarithm of the MADGRAPH matrix element computed using the constrained four-vectors of the b, the ℓ and the ν.
- ANN b-tag output.

B. t-channel Likelihood Function, 3 jet bin

The 3-jet bin t-channel likelihood function, $\mathcal{L}_t$, uses ten input variables. The algorithm used to select the b from top decay is as follows. If there is exactly one b-tagged jet in the event, it is used as the b from top decay. In events in which there are two or more tagged jets, only the leading two b-tagged jets are considered. The jet with the highest combination of $-\log\chi^2 + 0.005P_t$ is chosen, where χ^2 is the smaller of the two kinematic solver χ^2 outputs, one for each p_z solution of the neutrino, for combinations using that jet as the b from top decay. This algorithm assigns the correct jet to be the b from top decay approximately 75% of the time. The 3-jet bin t-channel likelihood function uses the following ten variables:

- $M_{\ell\nu b}$
- ANN b-tag output
- The number of b-tagged jets

– $q \times \eta$

– The smallest ΔR of any two jets

– M_{jj} of the two jets not chosen to be the b from top decay

– $\cos\theta_{t-\mathrm{chan}}$

– p_T of the lowest-E_T jet

– η of the reconstructed W boson

– p_T of the jet chosen to be the b from top decay

VI. SYSTEMATIC UNCERTAINTIES

Systematic variations in the rates and shapes of the likelihood distributions are considered for the signals and backgrounds in the sample. Systematic uncertainties contributing to the shape uncertainties are the jet energy scale (JES), initial state radiation (ISR) and final state radiation (FSR) variations, variations in the NN b-tag output distributions, variations in the flavor composition of the non-W sample, and variation in the Q^2 scale in ALPGEN. Shape uncertainties are also assessed for the mismodeling of the ΔR_{jj} and η_{j2} distributions, seen in the taggable-but-not-tagged samples. In the 3-jet bin,the ΔR_{jj} reweighted was not found to be needed. These same uncertainties contribute to the rate uncertainties, and additional contributions come from the uncertainty in the integrated luminosity, the parton distribution function used, the b-tag scale factor, the $t\bar{t}$ cross section prediction, and uncertainties propagated from the data-based background estimates. Tables II, III, IV V enumerate the relative rate errors on the backgrounds used in the limit calculations.

TABLE II: Fractional systematic rate uncertainties for the 2-jet 1 tag bin, in percent

Source	t-channel	s-channel	single-top	$t\bar{t}$
ISR less/more	2.8/-0.2	0.3/6.7	1.9/2.1	-2.6/-7.1
FSR less/more	4.2/-1.3	5.9/0.4	4.8/-0.7	-5.1/-2.6
PDF	3.4/-3.4	2.2/-2.2	3.0/-3.0	1.8/-1.8
MC	2.0/-2.0	1.0/-1.0	1.7/-1.7	-2.7/2.7
ϵ_{evt}	4.2/-4.2	2.3/-2.3	3.6/-3.6	2.9/-2.9
Luminosity	6.0/-6.0	6.0/-6.0	6.0/-6.0	6.0/-6.0
Cross section	12.6/-12.6	12.4/-12.4	12.6/-12.6	12.4/-12.4
M_{top} 170/180	1.3/-0.8	2.4/-1.7	1.7/-1.1	-3.1/1.4
	Diboson	Z+jets		
ϵ_{evt}	7.6/-7.6	8.3/-8.3		
Luminosity	6.0/-6.0	6.0/-6.0		
Cross Section	1.9/-1.9	10.8/-10.8		

TABLE III: Fractional systematic rate uncertainties for the 3-jet 1 tag bin, in percent

Source	t-channel	s-channel	single-top	$t\bar{t}$
ISR less/more	-6.8/-0.0	2.4/-12.6	-3.3/-4.8	-0.6/-4.6
FSR less/more	-1.5/-3.1	-6.0/-4.8	-3.3/-3.8	-3.4/-2.2
PDF	2.7/-2.7	2.3/-2.3	2.6/-2.6	1.8/-1.8
MC	1.9/-1.9	1.5/-1.5	1.7/-1.7	-1.7/1.7
ϵ_{evt}	3,5/-3.5	2.3/-2.3	3.0/-3.0	2.3/-2.3
Luminosity	6.0/-6.0	6.0/-6.0	6.0/-6.0	6.0/-6.0
Cross section	12.6/-12.6	12.4/-12.4	12.6/-12.6	12.4/-12.4
M_{top} 170/180	1.5/-2.8	6.0/-2.7	3.2/-2.7	-0.7/0.8
	Diboson	Z+jets		
ϵ_{evt}	7.8/-7.8	7.8/-7.8		
Luminosity	6.0/-6.0	6.0/-6.0		
Cross Section	1.9/-1.9	10.8/-10.8		

TABLE IV: Fractional Systematic rate uncertainties for 3-jet 2 tag bin, in percent

Source	t-channel	s-channel	single-top	$t\bar{t}$
ISR less/more	7.8/3.2	4.3/-11.2	5.8/-4.9	-0.5/-6.6
FSR less/more	15.0/1.3	-7.4/-5.0	2.4/-2.2	-3.4/-2.7
PDF	1.5/-1.5	2.1/-2.1	1.9/-1.9	1.7/-1.7
MC	1.9/-1.9	1.5/-1.5	1.7/-1.7	2.0/-2.0
ϵ_{evt}	9.1/-9.1	8.8/-8.8	8.9/-8.9	9.1/-9.1
Luminosity	6.0/-6.0	6.0/-6.0	6.0/-6.0	6.0/-6.0
Cross section	12.6/-12.6	12.4/-12.4	12.5/-12.5	12.4/-12.4
$M_{\rm top}$ 170/180	4.2/3.0	1.6/-6.8	2.7/-2.5	-0.6/-1.0
ϵ_{evt}	10.8/-10.8	11.1/-11.1		
Luminosity	6.0/-6.0	6.0/-6.0		
Cross Section	1.9/-1.9	10.8/-10.8		

TABLE V: Jet Energy Scale uncertainties, in percent

process	2jet 1 tag	3jet 1 tag	3jet 2 tag
t-channel	-1.1/0.6%	-10.4/10.6%	-5.7/4.3%
s-channel	-0.1-0.6%	-8.3/9.4%	-7.2/7.4%
$t\bar{t}$	9.8/-9.4%	4.6/-5.1%	-5.4/5.2%
$Wc\bar{c}$	7.0/-6.9%	8.4/-7.7%	11.0/-12.1%
$Wb\bar{b}$	7.0/-6.9%	8.4/-7.7%	11.0/-12.1%
Z+jets	-5.3/5.4%	-10.8/14.0%	-5.0/5.0%
diboson	-2.7/1.7%	-12.4/11.9%	-11.0/11.0%

VII. RESULTS

We use the likelihood functions described above to search for single-top quark production. We measure the single-top production cross section, using a Bayesian marginalization technique.

In order to measure the single-top production cross section, a Bayesian marginalization technique is applied to the t-channel likelihood output histograms in both the 2-jet and 3-jet samples. The Standard Model ratio between σ_s and σ_t and a flat prior in $\sigma_s + \sigma_t$ is assumed. The nuisance parameters are integrated out as described in [11],[7]. The distribution of the posterior is shown in Figure 4. The maximum of the posterior is taken to be the best-fit value, and the 68% confidence interval is taken to be the shortest interval containing 68% of the integral of the posterior distribution. The resulting cross section measurment is $\sigma_s + \sigma_t = 1.8^{+0.9}_{-0.8}$ pb.

Using the cross section measurement, we additionally measure $|V_{tb}| = 0.78^{+0.18}_{-0.21} \pm (0.07)$(theory), and set a limit of $|V_{tb}| > 0.41$ at 95% credibility level.

VIII. CONCLUSION

We present an analysis of the 2.2 fb^{-1} dataset in search of single-top-quark events, using a multivariate likelihood function technique, with a likelihood function designed to isolate t-channel signal events, and a separate likelihood function designed to isolate s-channel signal events.

The analysis proceeds on to a measurement of the single-top production cross section, assuming that the branching ratio $B(t \to Wb) \approx 100\%$, and that $M_t = 175$ GeV. Assuming further that the s-channel and t-channel cross sections obey their Standard Model theoretically predicted ratio, the single-top cross section is measured to be $\sigma_s + \sigma_t = 1.8^{+0.9}_{-0.8}$ pb. The Standard Model prediction for $\sigma_s + \sigma_t$ is $2.86^{+0.40}_{-0.33}$ pb [3] (The theory errors on σ_s and σ_t have been added linearly here, assuming they are 100% correlated).

Acknowledgments

We thank the Fermilab staff and the technical staffs of the participating institutions for their vital contributions. This work was supported by the U.S. Department of Energy and National Science Foundation; the Italian Istituto Nazionale di Fisica Nucleare; the Ministry of Education, Culture, Sports, Science and Technology of Japan; the Natural Sciences and Engineering Research Council of Canada; the National Science Council of the Republic of China; the Swiss National Science Foundation; the A.P. Sloan Foundation; the Bundesministerium für Bildung und Forschung, Germany; the Korean Science and Engineering Foundation and the Korean Research Foundation; the

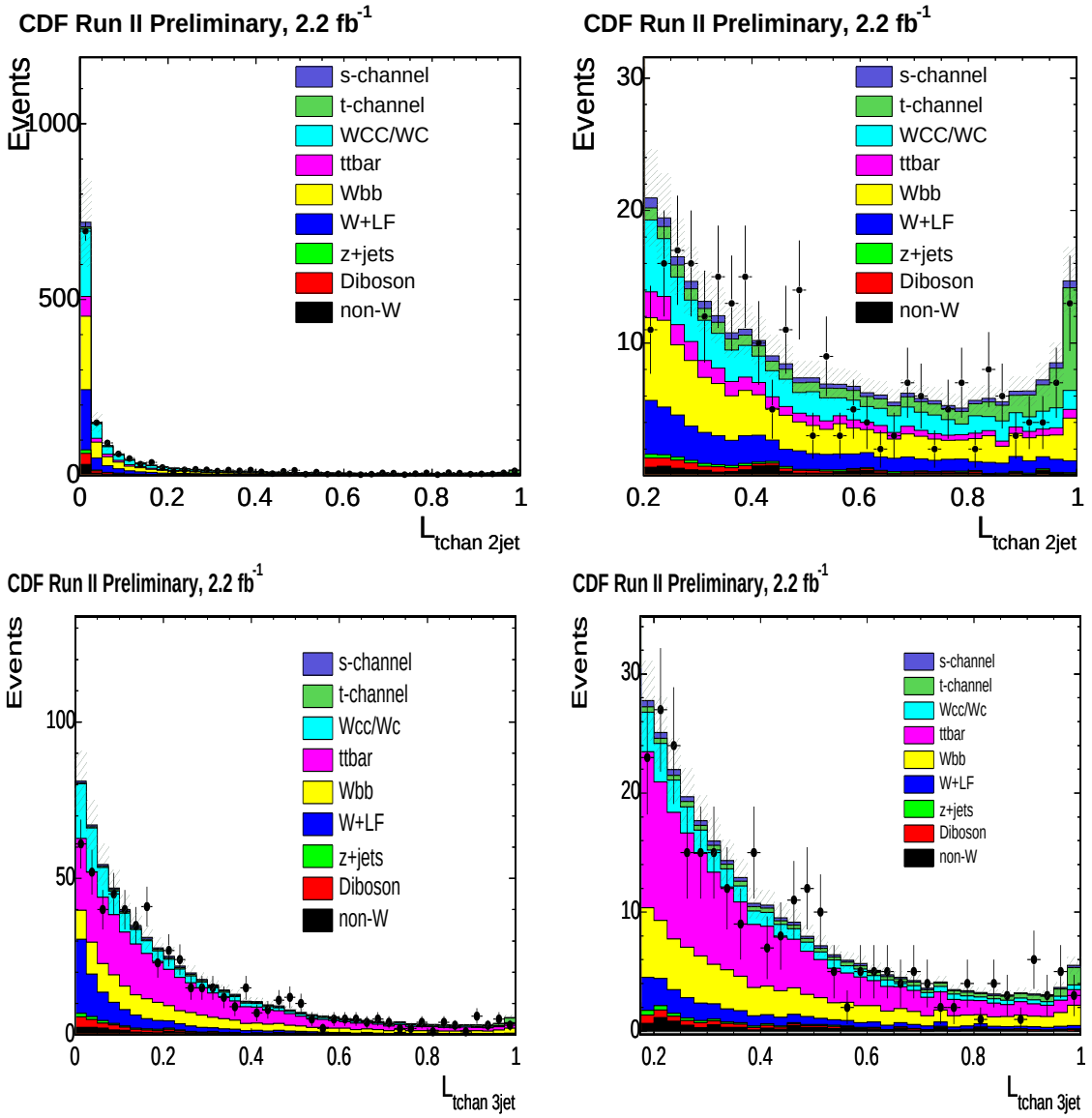

FIG. 3: The distributions of the t-channel 2-jet (upper) and 3-jet (lower) likelihood functions for CDF data compared to the Monte Carlo distributions normalized to the expected contributions. A linear (logarithmic) scale is used for the left (right) plots.

Science and Technology Facilities Council and the Royal Society, UK; the Institut National de Physique Nucleaire et Physique des Particules/CNRS; the Russian Foundation for Basic Research; the Comisión Interministerial de Ciencia y Tecnología, Spain; the European Community's Human Potential Programme; the Slovak R&D Agency; and the Academy of Finland.

[1] D. Acosta *et al.* (CDF Collaboration), Phys. Rev. D **65**, 091102 (2002); D. Acosta *et al.* (CDF Collaboration), Phys. Rev. D **69**, 052003 (2004); D. Acosta *et al.* (CDF Collaboration), Phys. Rev. D **71**, 012005 (2005).
[2] B. Abbott *et al.* (DØ Collaboration), Phys. Rev. D **63**, 031101 (2001); V. M. Abazov *et al.* (DØ Collaboration), Phys. Lett. B **517**, 282 (2001); V. M. Abazov *et al.* (DØ Collaboration), Phys. Lett. B **622**, 265 (2005).
[3] B. W. Harris *et al.*, Phys. Rev. D **66**, 054024 (2002); Z. Sullivan, Phys. Rev. D **70**, 114012 (2004).
[4] The CDF Collaboration, "Measurement of the Top Pair Production Cross Section in the Lepton+Jets Decay Channel" CDF Note 8795, 2007 (*public*)

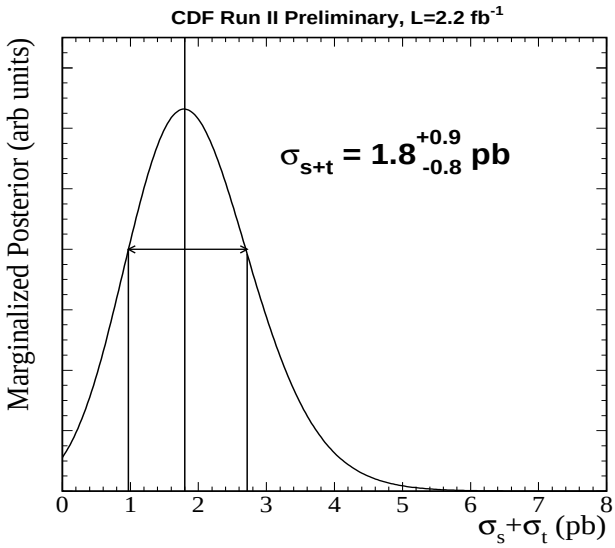

FIG. 4: Fit for $\sigma_s + \sigma_t$. A uniform prior in $\sigma_s + \sigma_t$ is assumed, and the SM ratio of σ_s/σ_t is also assumed. The Bayesian posterior, marginalized over nuisance parameters, is shown. The maximum value is the central value of the cross-section fit, and the smallest interval enclosing 68% of the integral of the posterior is the quoted interval. The measured result is $\sigma_s + \sigma_t = 1.8^{+0.9}_{-0.8}$ pb.

[5] T. Chwalek *et al.*, "Update of the Neural Network b Tagger for Single-Top Analyses", CDF note 8903, 2007 (*internal*).

[6] R. Barlow, "Statistics: a Guide to the Use of Statistics in the Physical Sciences" John Wiley and Sons, LTD, West Sussex, England (1989).

[7] T. Junk, "Sensitivity, Exclusion and Discovery with Small Signals, Large Backgrounds, and Large Systematics", CDF note 8128 (*internal*). Also see: A. L. Read, J. Phys. G: Nucl. Part. Phys. **28**, 2693 (2002); P. Bock *et al.* (the LEP Collaborations), CERN-EP-98-046 (1998) and CERN-EP-2000-055 (2000).

[8] M. Feindt, e-Print Archive physics/0402093 (2004).

[9] T. Tait and C. P. Yuan, Phys.Rev. **D63** (2001) 014018, available online as arXiv:hep-ph/0007298 (2000).

[10] Luc Demortier, Louis Lyons, Joel Heinrich, Giovanni Punzi, John Conway, Craig Blocker, Tom Junk, CDF Note 8023 (2006) (*internal*).

[11] J. Heinrich, "Bayesian limit software: multi-channel with correlated backgrounds and efficiencies", CDF note no. 7587 (*internal*).

[12] T. Tait and C. P. Yuan, Phys.Rev. **D63** (2001) 014018, available online as arXiv:hep-ph/0007298 (2000).

[13] V. M. Abazov *et al.* [D0 Collaboration], Phys. Rev. Lett. **98**, 181802 (2007) [arXiv:hep-ex/0612052];
`also see: http://www-d0.fnal.gov/Run2Physics/top/top_public_web_pages/top_public.html`

[14] M. Buehler *et al.*, "Search for Electroweak Single-Top-Quark Production using Neural Networks with 955 pb-1 of CDF", CDF Note 8677, 2007 (*public*);
S. Budd *et al.*, "Search for Single-Top-Quark Production Using a Multivariate Likelihood Technique", CDF Note 8585, 2007 (*public*);
F. Canelli*et al.*, "Search for Single-Top-Quark Production in 955 pb-1 using the Matrix Element Technique", CDF Note 8588, 2007 (*public*)
also see: http://www-cdf.fnal.gov/physics/new/top/top.html

[15] `see: http://www-cdf.fnal.gov/physics/new/top/2007/singletop/LF1_5fb/LF1_5fb_Public_page.html`